Article published online: 2021-05-10

AIMS Genetics

http://www.aimspress.com/journal/Genetics

AIMS Genetics, 3(4): 239-251.
DOI: 10.3934/genet.2016.4.239
Received: 29 August 2016
Accepted: 11 November 2016
Published: 16 November 2016

Research article

Thymoquinone disrupts the microtubule dynamics in fission yeast *Schizosaccharomyces pombe*

Nusrat Masood[1], Saman Khan[2], Suaib Luqman[1,*] and Shakil Ahmed[2,*]

[1] Molecular Bioprospection Department of Biotechnology Division, CSIR-Central Institute of Medicinal and Aromatic Plants, Lucknow-226015, Uttar Pradesh, India.
[2] Molecular and Structural Biology Division, CSIR—Central Drug Research Institute, Sector 10, Jankipuram Extension, Sitapur Road, Lucknow-226031, India,

* **Correspondence:** Email: shakil_ahmed@cdri.res.in, s.luqman@cimap.res.in;
Tel: +91-522-2771940, ext 4453; Fax: +91-522-2771941.

Abstract: Mad2 deletion strain of *Schizosaccharomyces pombe* was found to be sensitive to thymoquinone, a signature molecule present in *Nigella sativa* in a dose-dependent manner. Mad2 protein is an indispensable part of mitotic spindle checkpoint complex and is required for the cell cycle arrest in response to the spindle defects. Although the expression of α tubulin was not affected in thymoquinone treated cells, but the expression of β-tubulin was reduced. Further, the absence of microtubule in thymoquinone treated cells suggests its involvement in tubulin polymerization. Molecular docking studies revealed that thymoquinone specifically binds to β-tubulin near the Taxotere binding site of Tub1 (Tubulin α-β dimer). These studies additionally showed that thymoquinone interacts with the residues present in chain B, which is an inherent part of Mad2 protein of mitotic checkpoint complex (MCC). We concluded that the thymoquinone disrupts the microtubule polymerization that leads to the requirement of spindle checkpoint protein for the cell survival.

Keywords: Thymoquinone; spindle assembly checkpoint; Mad2; Tubulin

1. Introduction

Schizosaccromyces pombe come up to an elevated level of perpetuation in cellular processes mimicking mammalian cells with numerous advantages including simple growth requirements, rapid cell division and ease of genetic maneuvring [1]. Cell cycle checkpoints are inherent safety guard of the cell warranting proper growth, and defect in these cell cycle checkpoints can lead to the tumor

progression. Spindle Assembly Checkpoint (SAC), Centrosome Duplication Checkpoint (CDC) and DNA Damage Checkpoint are the major checkpoints operating during the cell cycle progression [2-6]. SAC is a conserved surveillance mechanism that arrests cells in mitosis in response to malfunctioning spindle [7]. SAC prevents the anaphase onset, mitosis exit, cytokinesis initiation and is triggered by either existence of unattached kinetochore or by the lack of tension on kinetochores [8,9]. The core proteins involved in SAC are Bub1, Bub3, Mad1, Mad2 and Mad3 [10,11]. These proteins are responsible for regulating Anaphase Promoting Complex (APC) activity. APC inhibition takes place after the suppression of the Cdc20 (APC activator) by Mad2, thereby averting premature cyclin B and securin degradation [12-14]. The *S. pombe* SAC protein Mad2 interacts with APC and blocks anaphase. In response to the defective microtubule, the Mad2-dependent SAC delays mitotic exit [10]. In *S. pombe*, Mad2 over-expression imitates activation of the SAC and results in the arrest of cell cycle at the metaphase-anaphase transition [15,16]. Tumor cells frequently exhibit Chromosomal Instability (CIN) instead of undergoing apoptosis and endure a convinced level of aneuploidy. During development and aging, polyploidy is programmed in selected tissues but sometimes due to stress and particular disease condition like cancer, random polyploidization occurs [17]. Inhibition of Mad2 or BubR1 checkpoint proteins in aneuploid cancer cells restrains pathways necessary to maintain CIN [18].

Thymoquinone (TQ) is a mitochondria-targeted antioxidant, anti-inflammatory, antineoplastic agent that regulates apoptosis by either amending PI3K/Akt and p38kinase pathways or by inducing ROS generation [19,20]. TQ affects the α/β tubulin degradation with upregulation of tumor suppressor p73 and G2/M phase apoptosis in U87 astrocytoma cancer cells and Jurkat T-lymphoblastic leukemia cells with no effects in normal fibroblast cells suggesting its role as an anti-microtubule drug [21]. In this report, cell cycle checkpoint inhibition was studied with selected monoterpenes present in many plants including *Nigella sativa*. We reported that the thymoquinone (TQ) disrupts the microtubule assembly that leads to growth inhibition in spindle checkpoint defective mutants. Furthermore, *in silico* studies revealed that TQ specifically binds to β-tubulin and mitotic checkpoint complex (MCC) through chain B, which is an inherent part of Mad2 protein.

2. Material and Methods

2.1. Chemicals, biochemicals, and reagents used

Yeast Extract, Agar Powder, Adenine, Tris-base, EDTA were obtained from HiMedia, India. β-mercaptoethanol, EDTA, Pyridoxal phosphate, L-Ornithine HCl, Sodium hydroxide, 1- Pentanol, Sodium Borate, TNBS, DMSO, β-NADPH, Di potassium hydrogen phosphate and Potassium dihydrogen phosphate, Thymoquinone were obtained from Sigma-Aldrich, India. Stock solution of thymoquinone (10 mg/mL) was prepared in DMSO and final working concentration used was 10 μg/mL, 20 μg/mL, and 30 μg/mL.

2.2. Yeast strains and growth conditions

Haploid wild-type (SP6: *h⁻leu-32*), *mad2* deletion (NW1419: *h⁻leu1-32 ura4DS/E mad2::ura4 ade6-210*) and *bub1* deletion (SH495*: h⁻* leu1-*32 bub1::kan*^{R}) strains of *S. pombe* were used. For the spotting experiment, wild type and *mad2* deleted strains were grown at 30 °C up to mid-log phase, 10^7 cells were serially diluted, spotted on plates containing thymoquinone and incubated at 30 °C for 3 days before taking photographs. For cell survival assay, wild-type and *mad2* deleted strains

were grown in the presence of different concentrations of thymoquinone for 2 h at 30 °C, for each sample ~1000 cells were placed on YEA plates and incubated at 30 °C until colonies appear. A graph was plotted after colony count.

2.3. Preparation of cell lysate and western blot analysis

Cells were grown to mid-log phase and shifted to YEA media containing no drug or 30 µg/mL thymoquinone, incubated at 30 °C for 2 h. Cells were harvested by centrifugation and lysed using glass beads and a Fast Prep (Bio 101) vortex machine. Lysate in Phosphate Buffered Saline (PBS) was centrifuged at 10000 rpm in a microfuge for 5 min at 4 °C. Protein was estimated from the supernatant collected using Bradford assay. For western blot analysis, about 200 µg of total cell lysate was run on 10% SDS-PAGE, transferred to a nitrocellulose membrane, probed with anti-α-tubulin or anti β-tubulin antibody and horseradish peroxidase (HRP) -conjugated anti-mouse antibody. ECL western blotting detection reagents (Pierce) were used for protein detection using hyper film ECL (GE healthcare).

2.4. Immunofluorescence studies

Exponentially growing cells already treated with thymoquinone were used for immunofluorescence studies as described previously [22]. The cells were fixed with freshly prepared 3.7% formaldehyde for 30 min with shaking, washed by PEM buffer for 3 times and spheroplasting was performed using zymolyase. Primary antibody (Anti α-tubulin) was used at a dilution of 1:50, incubated overnight at room temperature. Cells were washed, treated with FITC-conjugated secondary antibody at a dilution of 1:100 and incubated for 4 h at room temperature. Analysis of the cells was done using a fluorescence microscope and processing was performed by Adobe Photoshop.

2.5. In silico docking studies

To comprehend the interactions of Thymoquinone with MCC, docking studies were performed. The 3D structures of Thymoquinone (CID_10281) were retrieved from PubChem database at NCBI web server (http://pubchem.ncbi.nlm.nih.gov). X-ray crystallographic 3D structures of Tubulin α-β dimer (PDB ID: Tub1) and Mitotic checkpoint complex of *S. pombe* (PDB ID: 4AEZ) were retrieved from Brookhaven Protein Data Bank (http://www.pdb.org). Docking was executed by using AutoDock 1.5.4 software [23] as the version uses the Lamarckian Genetic Algorithm and empirical free energy scoring function, typically providing reproducible docking results for ligands with approximately 10 flexible bonds. AutoDock 1.5.4 uses a semiempirical free energy force field to evaluate conformations in terms of inhibition constant (Ki) and binding energy (B.E.) during docking simulations. The docked proteins were visualized through UCSF Chimera, version 1.6. [24] Also to understand the association between H-bonding and hydrophobic interactions, Ligplot 1.4.5 (http://www.ebi.ac.uk/thrntosrv/software/LIGPLOT/) was used to engender schematic diagrams of protein-ligand interactions [25].

2.6. Statistical analysis

Experiments were executed in duplicate each time and values are mean ± SD of three independent analyzes. Results were subjected to analysis of variance (ANOVA), and differences between means at $p < 0.05$ level were considered significant compared to control in student's *t*-test.

3. Results

3.1. TQ affects the spindle assembly checkpoint

Some checkpoint deficient mutant/knockout strains of *S. pombe* were assayed for their ability to grow on the plates containing TQ. Cells containing *mad2* and *bub1* deletion were found to be more sensitive than the wild-type strains at 20 and 30 µg/mL concentration (Figure 1A). While *chk1* and *cds1* deletion strains do not exhibit such growth defect suggesting that abrogation of only spindle assembly checkpoint and not DNA damage checkpoint response or S phase checkpoint response affect cell survival in response to thymoquinone. Furthermore, only 18% *mad2*Δ cells were able to form colonies at 20 µg/mL concentration after 2 h exposure with TQ. The survival of *mad2*Δ cells was further reduced to 1.6% at 30 µg/mL concentration (Figure 1B). Similarly the survival of *bub1Δ* cells was reduced to 13% and 0.8% at 20 and 30 µg/mL concentration of thymoquinone respectively (Figure 1B). In contrary, the survival of wild-type cells was 83% and 45% at 20 and 30 µg/mL concentration respectively suggesting a dose-dependent inhibition of growth in *mad2*Δ and *bub1Δ* cells. As a control, the sensitivity of *mad2Δ* and *bub1Δ* strain on a plate containing thiabendazole (TBZ), a known microtubule inhibitor has also been shown (Figure 1A, last panel).

3.2. The expression of β-tubulin was reduced after treatment with thymoquinone

Earlier studies suggest the involvement of thymoquinone in the degradation of α/β tubulin in cancer cell line [21]. Further to elucidate whether the growth defect in *mad2*Δ was due to the differential expression of tubulin protein, an important component of the microtubule, we performed western blot analysis after treating the wild type and *mad2*Δ cells with 30 µg/mL of TQ for 2 h. As presented in Figure 2A, the expression of α-tubulin was not affected in wild-type as well as in *mad2*Δ strain (data not shown) suggesting that TQ does not influence the expression of α-tubulin. Interestingly the expression level of β-tubulin was reduced after exposing the cells to thymoquinone for 2 h (Figure 2B) that might be due to the degradation of β-tubulin protein as has also been reported in cancer cell line [21].

3.3. Thymoquinone disrupts spindle microtubule dynamics

Since the growth of *mad*2Δ cells was inhibited after treatment with TQ, we hypothesized that these phyto molecules might be affecting the formation of the microtubule network. In order to analyze this possibility, we performed immunofluorescence studies in the cells treated with 30 µg/mL of TQ for 2 h. The wild type untreated cells exhibited typical elongated microtubule structure (Figure 2C, left panel). Interestingly, these microtubule structures were absent in the cells treated with TQ (Figure 2C, right panel) clearly indicating that thymoquinone might be affecting the formation of microtubule structure.

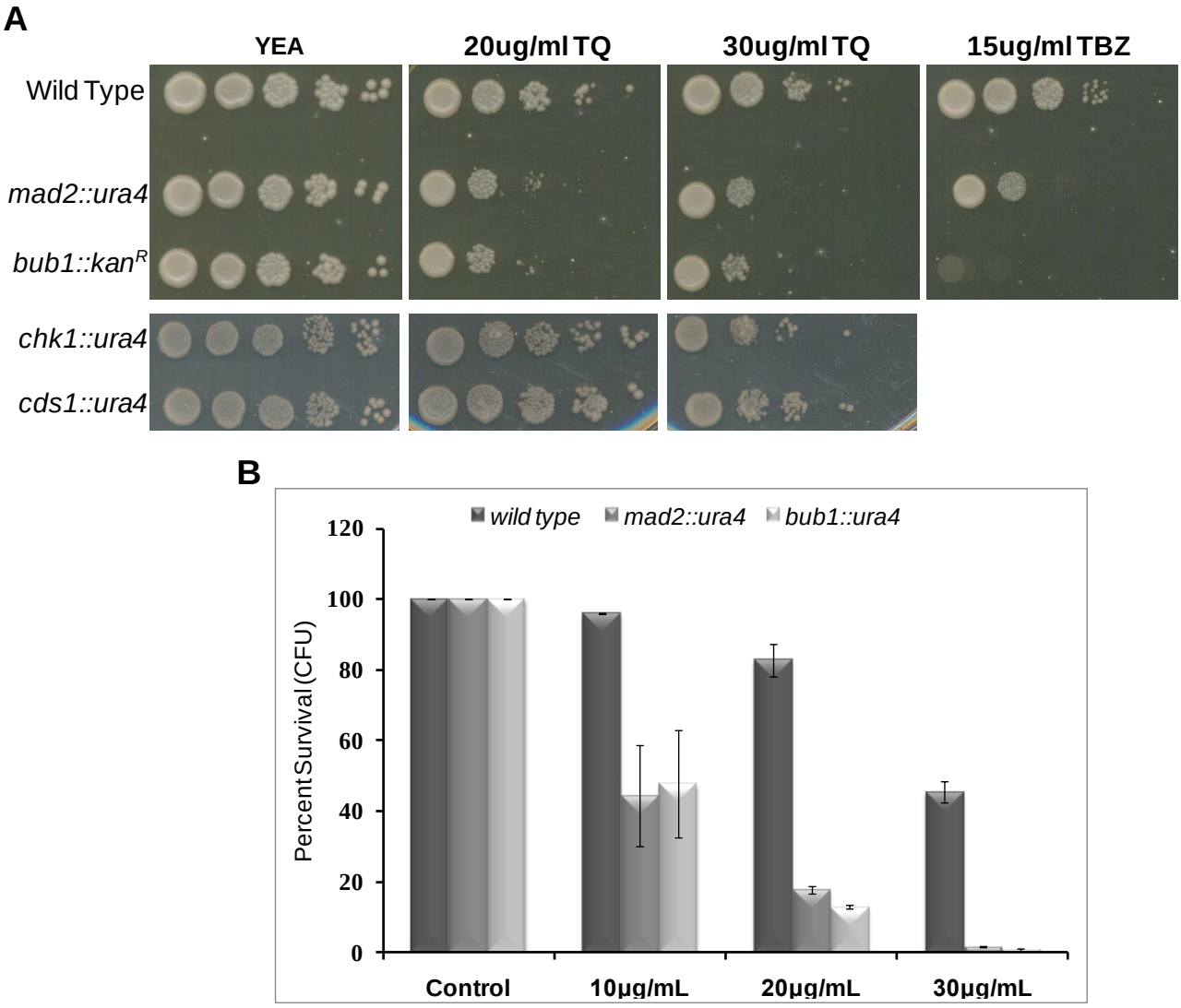

Figure 1. *mad2* and *bub1* deleted cells exhibit sensitivity towards thymoquinone. (A) Indicated strains were grown to mid-log phase, 10 fold serial dilutions were spotted on the rich media plate containing indicated doses of thymoquinone. The thiabendazole (TBZ) sensitivity of *mad2* deleted and *bub1* deleted cells was also shown. (B) Indicated strains were allowed to grow in the presence of indicated doses of thymoquinone for 2 h. An equal number of the cells from each sample were plated on rich media plates, and plating efficiency was calculated. All data are the mean of three independent experiments. Statistical significance test was done through GraphPad Instat Version 3.10 by One-way Analysis of Variance (ANOVA) specifically through Dunnett Multiple Comparisons Test.

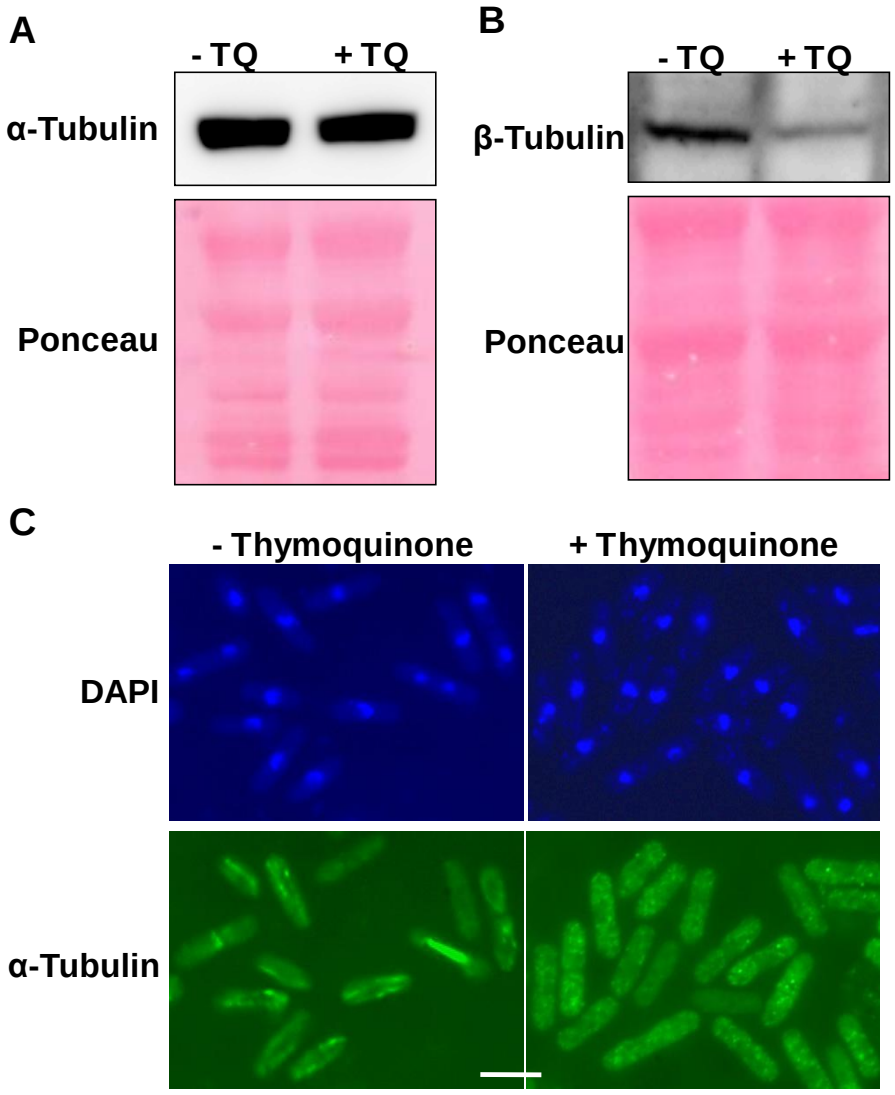

Figure 2. The expression level of α and β-tubulin in response to thymoquinone. The wild-type cells were grown to mid-log phase in the presence or the absence of thymoquinone, the lysate was prepared, and western blot analysis was performed using (A) anti α- tubulin and (B) anti-β-tubulin antibody. Pictures of ponceau stained gel were shown as loading control. (C) Wild-type cells grown in presence or absence of thymoquinone were processed for indirect immunofluorescence using anti α-tubulin antibody. Nuclei were stained with DAPI. Scale bar: 10 µm.

3.4. In silico docking analysis showed that thymoquinone interacts with β-tubulin and Mad2

TQ was docked with Tubulin α-β heterodimer [Tub1] consisting of 2 chains which are represented by 2-sequence unique entities. Chain A consists of tubulin α subunit [d1tuba1 and d1tuba2] and in this subunit there is a binding site for non-exchangeable GTP. Chain B consists of tubulin β subunit [d1tubb1 and d1tubb2] and in this subunit there is a binding site for exchangeable GTP, GDP, and Taxotere (TXL). Binding energy estimated for TQ docked with

Tub1 was −7.2 kcal/mol and inhibition constant was 5.25 µM. Selected residues of Tub1 surrounding TQ within the range of 4Å were Val 23.B, Asp 26.B, Glu 27.B, His 28.B, Tyr 36.B, Thr 240.B, Phe 244.B, Arg 320.B, Ile 358.B, Pro 359.B, Pro 360.B, Arg 369.B and TXL 501.B (TXL). It means that residues present surrounding the docked ligand belongs to chain B which corresponds to tubulin β subunit and also it is in close proximity to taxol binding site. Common residues which were present surrounding 4Å of taxol and TQ include Val 23.B, Asp 26.B, Arg 320.B, Pro 360.B, Arg 369.B (Figure 3A, B, C).

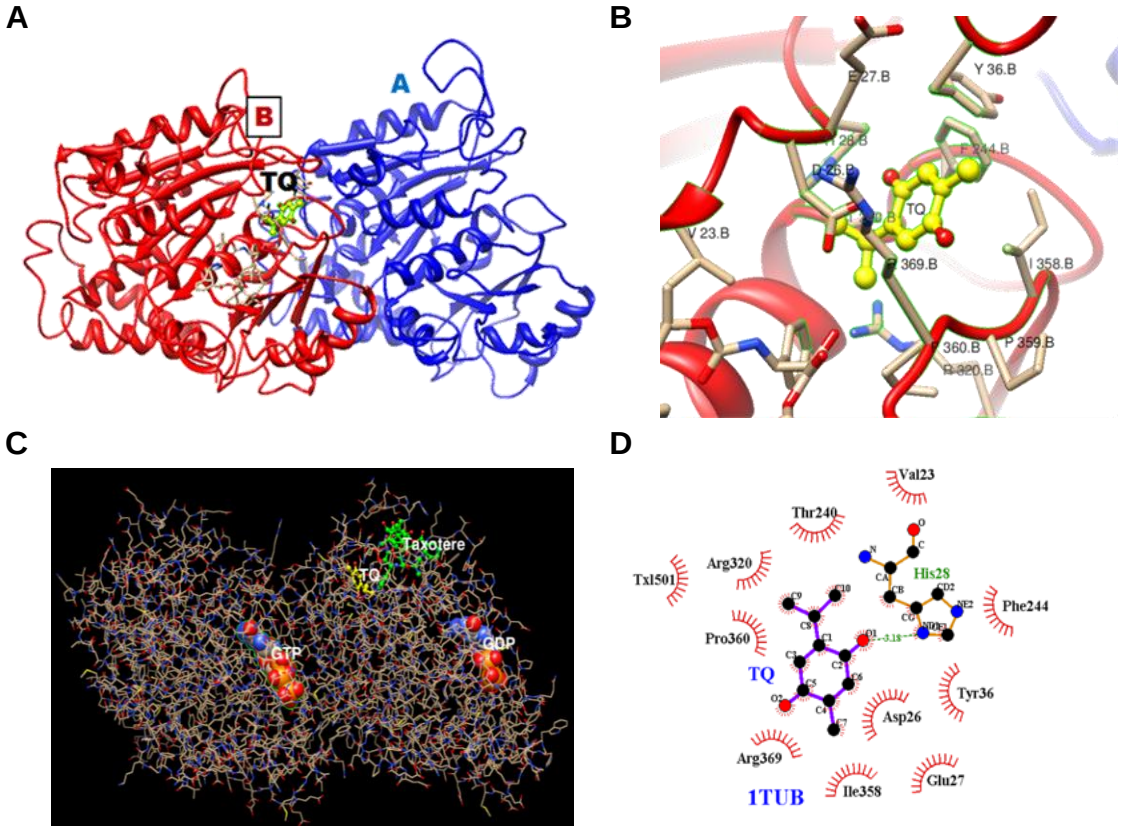

Figure 3. Molecular docking studies of thymoquinone with the Tubulin α-β heterodimer [Tub1]. (A) Structural overview of the Tubulin α-β dimer [Tub1] with TQ docked complex. The Tubulin-αβ heterodimer was downloaded from Protein Data Bank, and the ligand i.e., thymoquinone was taken from PubChem, docking was performed using software Autodock 1.5.4. The Tub1 dimer consists of α protein shown in blue and β protein shown in red while TQ is displayed in yellow. (B) A close-up of the docked protein displaying the residues involved within 4Å zone and was visualized through UCSF Chimera, version 1.6. (C) The relative spatial location of TQ, Taxotere, GDP and GTP in tubulin heterodimer [Tub1] visualized through UCSF Chimera, version 1.6. (D) Ligplot diagram of TQ docked with Tub1 (Ligplot 1.4.5) showing hydrogen bonds between the oxygen of C2 of TQ with His 28 with donor-acceptor distance of 3.18 Å. The interactions shown are those mediated by hydrogen bonds (green) and by hydrophobic contacts (red). Hydrogen bonds are indicated by dashed lines between the atoms involved while hydrophobic contacts are represented by an arc with spokes radiating towards the ligand atoms they contact.

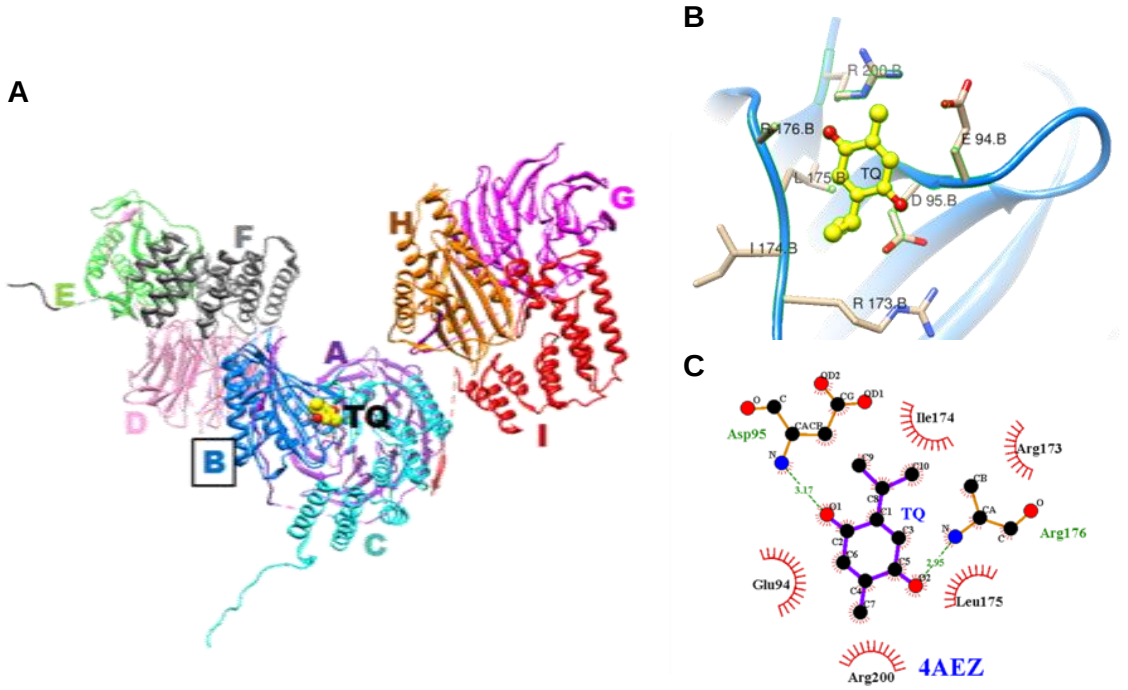

Figure 4. Molecular docking studies of thymoquinone with the mitotic checkpoint complex protein of *S. pombe* [4AEZ]. (A) Structural overview of the mitotic checkpoint complex protein of *S. pombe* [4AEZ] with TQ docked complex. The mitotic checkpoint complex was downloaded from Protein Data Bank, and the ligand i.e., thymoquinone was taken from PubChem, docking was performed using software Autodock 1.5.4. The MCC complex protein is a trimer consisting of WD repeat-containing protein Slp1 [chains: A, D, G]; Mad2 [chains: B, E, H] and Mad3 [chains: C, F, I]. The Mad2 protein represented by chain B (Blue), chain E (green) and chain H (orange). The ligand (TQ) displayed in yellow docks with the MCC complex at chain B, which is inherent of Mad2 protein. (B) Focussed docked protein with ligand (TQ) surrounded by residues within the 4Å area by UCSF Chimera 1.6. (C) Ligplot diagram of TQ docked with 4AEZ (Ligplot 1.4.5) showing hydrogen bonds between the oxygen of C2 of TQ with Asp 95 with donor-acceptor distance of 3.17 Å and between the oxygen of C5 of TQ with Arg 176 with donor-acceptor distance of 2.95 Å. The interactions shown are those mediated by hydrogen bonds (green) and by hydrophobic contacts (red). Hydrogen bonds are indicated by dashed lines between the atoms involved while hydrophobic contacts are represented by an arc with spokes radiating towards the ligand atoms they contact.

We also docked TQ with AEZ (crystal structure of MCC of *S. pombe*) which consists of 3 proteins (hetero-trimer): [Slp1, Mad2 dimer, Mad3 trimer] and 9 chains in the complex. Chains corresponding to Slp1 protein are Chain A, D, G. Chains corresponding to Mad2 protein are Chain B, E, H and lastly chains corresponding to Mad3 protein are Chain C, F, I [26]. Selected residues surrounding TQ docked with protein AEZ within the range of 4Å comprised of Glu 94.B, Asp 95.B, Arg 173.B, Ile 174.B, Leu 175.B, Arg 176.B and Arg 200.B (Figure 4B). It means that residues present surrounding the docked ligand belongs to chain B which corresponds to Mad2 protein. Binding energy estimated for TQ docked with 4AEZ was −4.61 kcal/mol and inhibition constant was

414.71 µM (Figure 4A, B). Other spindle poison TBZ does not shows any affinity with Mad2 protein but it does interacts with Slp1 and Mad3 protein within MCC complex (data not shown) suggesting that binding of spindle poison with MCC complex might also affect the cell survival in response to spindle poison.

Crystal Structure of Mitotic Checkpoint Complex (PDB: 4AEZ) containing Mad2, Mad3 and Slp1 of *S. pombe* is available while the Bub1 protein is not available for *S. pombe*, instead there is a *Saccharomyces cerevisiae* protein structure of Bub3-Bub1 bound to phospho-Spc105 (PDB: 4BL0). We docked our ligand, TQ with this protein and the B.E. and Ki are −6.38 kcal/mol and 21.14 µM respectively (Figure 5A). The docked residues were: GLN 8.A, ALA 9.A, PRO 10.A, LYS 11.A, ASP 32.A, SER 34.A, THR 36.A, TYR 38.A and LYS 11.D (Figure 5B). In this the A and D represents the chain while the number represents the position of the residue. This protein complex (PDB ID: 4BL0) consists of 3 proteins: Bub3 (chain A, D); Bub1 (chain B, E) and Spc105 (chain C, F) (Figure 5A). Thus it is clear that TQ binds to Bub3 and not with Bub1 in protein complex (Figure 5). Further fission yeast Bub3 is required for normal spindle dynamics, but not for SAC [27]. Bub1 is a fission yeast kinetochore scaffold protein, and is sufficient to recruit other spindle checkpoint proteins to ectopic sites on chromosomes [28]. Thus in fission yeast spindle assembly checkpoint complex, TQ binds and affects only Mad2 and does not affect other proteins necessary for spindle assembly checkpoint. These results suggest that the growth defects observed in *bub1Δ* strain (Figure 1A) might be due to the defects in the microtubule polymerization.

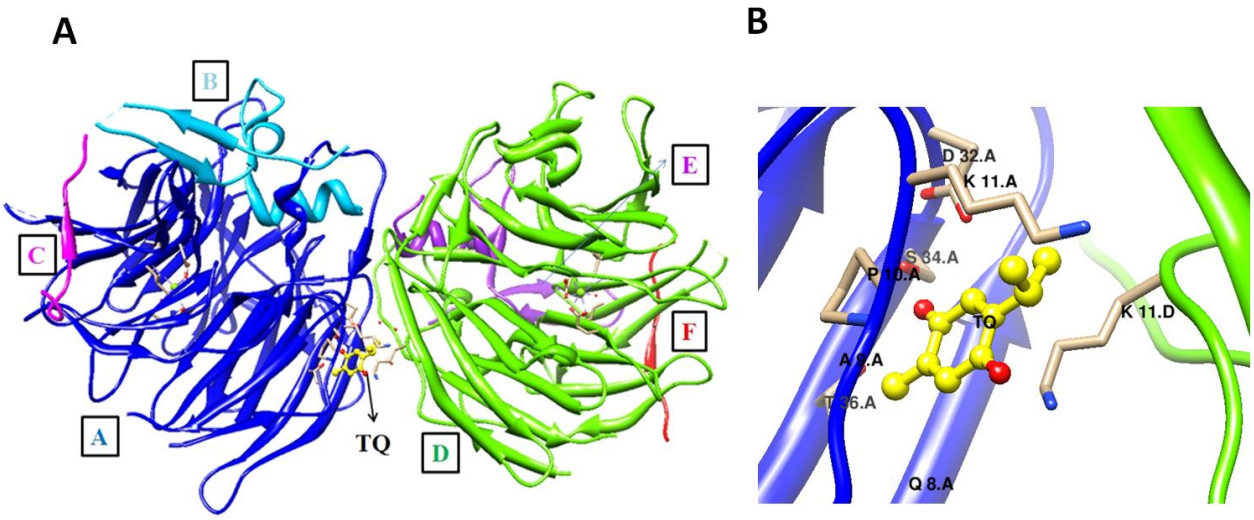

Figure 5. Molecular docking studies of thymoquinone with the Bub3 in complex with Bub1 and Spc105 (A) Structural overview of the Bub1-Bub3-Spc105 protein complex with TQ docked complex. **(B)** A close-up of the docked Bub3 protein with TQ displaying the residues involved within 4Å zone by UCSF Chimera, version 1.6.

3.5. Effect of Mad2 over-expression was not affected by thymoquinone

Mad2 over-expression leads to the metaphase arrest and hence cells are unable to complete the cell division that affects its survival [29]. In order to check the role of thymoquinone on the over-expression of *mad2*, we checked the survival of *mad2* over-expressing cells under the thiamine

repressible promoter in the presence of thymoquinone. As shown in Figure 6, cells containing *mad2* gene under thiamine repressible *nmt* promoter were growing well in the presence of thiamine but in the absence of thiamine these cells were unable to form colonies due to the over- expression of *mad2* gene. We found there was no change in the survival of *mad2* over-expressing cells when thymoquinone was added to the media (Figure 6). While cells containing vector control were growing well on all the plates (Figure 6). These results suggest that the binding of TQ with the proteins required for spindle assembly checkpoint pathway (Mad2 and Bub3) might be responsible for growth defect. Alternatively, binding of TQ with tubulin leads to the requirement of these proteins for proper cell division and in the absence of proper spindle assembly checkpoint function cell survival is affected.

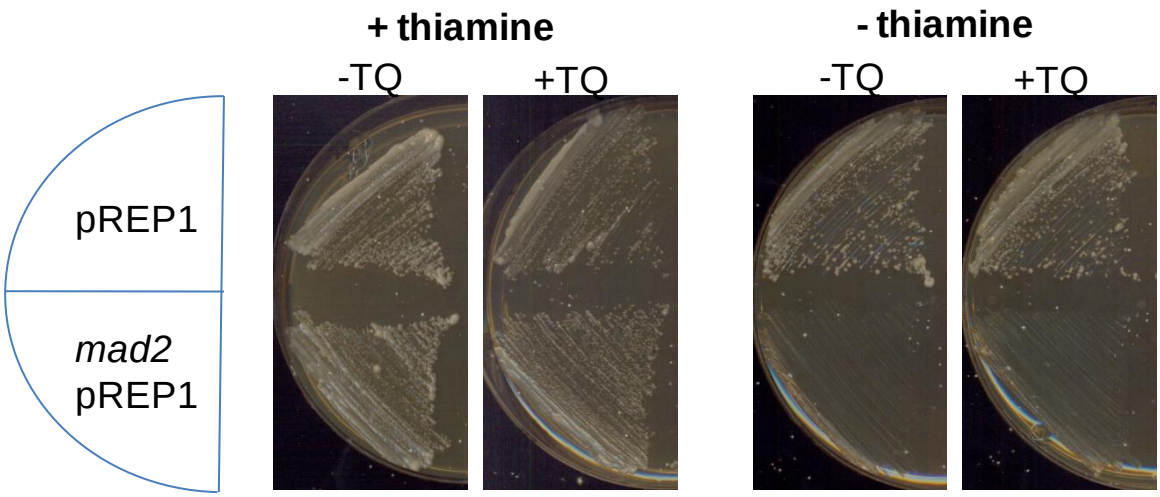

Figure 6. *mad2* over-expression studies in response to thymoquinone. Plasmid containing *mad2* gene under thiamine repressible *nmt* promoter along with vector control was transformed in wild type cells. Transformants were streaked on plate containing thiamine and thymoquinone as indicated. Plated were incubated at 30 °C for 4 days before taking photograph.

4. Conclusion

Yeast cells mimic eukaryotic mammalian cells in their mechanism while being unicellular and application of genetic approach ultimately helps to study the complex cellular function. Using phenotype-based screens the yeast model system can lead us to identify the exact mechanism of how a chemical inhibitor works within the cell [1]. In order to identify the potential target of thymoquinone, we studied the growth inhibition of some deletions or mutant strains of fission yeast *S.pombe* (particularly cell cycle checkpoint mutants) in the presence of thymoquinone. A dose-dependent inhibition of growth in *mad2*Δ cells by thymoquinone was observed indicating poor survival in response to TQ in the absence of functional SAC. Mad2 is a key component of the SAC that delays the start of anaphase until all kinetochores are attached to the spindle [30]. It attaches to Cdc20, a co-activator of APC or cyclosome and prevents it from advancing destruction of securin [31,32]. In yeast, microtubules are a critical component of the mitotic spindle that split the genetic material during cell division. We also observed that the expression of β-tubulin was affected in thymoquinone treated cells and the microtubule assembly was impaired. We hypothesized that due to the defective

microtubule structure the *mad2Δ* and *bub1Δ* cells were unable to grow in the presence of thymoquinone since these cells required a functional spindle checkpoint for their survival.

Microtubules are formed by heterodimers of alpha and beta tubulin subunits in a 1:1 ratio. *In silico* docking studies indicated that thymoquinone binds to β-tubulin of αβ tubulin dimer near the Taxotere binding site that strengthen our hypothesis that a sophisticated system of microtubule formation and dissociation was affected by thymoquinone. Recently, thymoquinone has been reported as a new anti-microtubule agent in cancer cell lines. In the presence of thymoquinone a concentration and time-dependent degradation of α/β tubulin has been reported in A87 and Jurkat cell lines while no effect was observed in normal human fibroblast cells [21]. Further it has been observed that thymoquinone depolymerizes the microtubule network of A549 cells [33]. The tubulin polymerization in the presence of thymoquinone was also inhibited in a cell-free system with an IC_{50} value of 27 μM [34]. Most of the anti-mitotic drugs like Paclitaxel, Vincristine, Colchicine itself binds to β-tubulin and ultimately disrupts the equilibrium [33]. The present finding indicating the reduced survival of SAC compromised cells in response to TQ could be responsible for driving the tumour cells towards apoptosis and hence impart the anticancer activity.

Acknowledgments

We are grateful to Council of Scientific and Industrial Research (CSIR), New Delhi for Senior Research Fellowship to NM and Indian Council of Medical Research Fellowship for SK. This study was supported by the grant from Council of Scientific and Industrial Research (BSC0103 and BSC0121), New Delhi, India. The CDRI communication number for this manuscript is 9377.

Conflict of interest

The authors declare there is no conflict of interest.

References

1. Simon JA, Bedalov A (2004) Yeast as a model system for anticancer drug discovery. *Nat Rev Cancer* 4: 481-487.
2. Habu T, Matsumoto T (2013) p31 (comet) inactivates the chemically induced Mad2-dependent spindle assembly checkpoint and leads to resistance to anti-mitotic drugs. *Springer Plus* 2: 562.
3. Elledge SJ (1998) Mitotic arrest: Mad2 prevents sleepy from waking up the APC. *Science* 279: 999-1000.
4. Kops GL, Weaver BA, Cleveland DW (2005) On the road to cancer: aneuploidy and the mitotic checkpoint. *Nat Rev Cancer* 5: 773-785.
5. Nasmyth K (2005) How do so few control so many? *Cell* 120: 739-746.
6. Page BD, Snyder M (1993) Chromosome segregation in yeast. *Annu Rev Microbiol* 47: 231-261.
7. Amon A (1999) The spindle checkpoint. *Curr Opin Genet Dev* 9: 69-75.
8. Lew DJ, Burke DJ (2003) The Spindle Assembly and Spindle Position Checkpoints. *Annu Rev Genet* 37: 251-282.
9. Pinsky BA, Biggins S (2005) The spindle checkpoint: tension versus attachment. *Trends Cell Biol* 15: 486-493.
10. Li R, Murray AW (1991) Feedback control of mitosis in budding yeast. *Cell* 66: 519-531.

11. Hoyt MA, Totis L, Roberts BT (1991) *S. cerevisiae* genes required for cell cycle arrest in response to loss of microtubule function. *Cell* 66: 507-517.
12. Foley EA, Kapoor TM (2013) Microtubule attachment and spindle assembly checkpoint signalling at the kinetochore. *Nat Rev Mol Cell Biol* 14: 25-37.
13. Schweizer N, Ferras C, Kern DM, et al. (2013) Spindle assembly checkpoint robustness requires Tpr-mediated regulation of Mad1/Mad2 proteostasis. *J Cell Biol* 203: 883-893.
14. Musacchio A, Salmon ED (2007) The spindle-assembly checkpoint in space and time. *Nat Rev Mol Cell Biol* 8: 379-393.
15. He X, Jones MH, Winey M, et al. (1998) Mph1, a member of the Mps1-like family of dual specificity protein kinases, is required for the spindle checkpoint in S. pombe. *J Cell Sci* 111: 1635-1647.
16. He X, Patterson TE, Sazer S (1997) The Schizosaccharomyces pombe spindle checkpoint protein mad2p blocks anaphase and genetically interacts with the anaphase-promoting complex. *Proc Natl Acad Sci USA* 94: 7965-7970.
17. Rajagopalan H, Lengauer C (2004) Aneuploidy and cancer. *Nature* 432: 338-341.
18. Pandit SK, Westendorp B, de Bruin A (2013) Physiological significance of polyploidization in mammalian cells. *Trends Cell Biol* 23: 556-566.
19. Severina II, Severin FF, Korshunova GA, et al. (2013) In search of novel highly active mitochondria-targeted antioxidants: thymoquinone and its cationic derivatives. *FEBS Lett* 587: 2018-2024.
20. Yu SM, Kim SJ (2013) Thymoquinone-induced reactive oxygen species causes apoptosis of chondrocytes via PI3K/Akt and p38kinase pathway. *Exp Biol Med* 238: 811-820.
21. Alhosin IM, Ibrahim A, Boukhari A, et al. (2012) Anti-neoplastic agent thymoquinone induces degradation of alpha and beta tubulin proteins in human cancer cells without affecting their level in normal human fibroblasts. *Invest New Drugs* 30: 1813-1819.
22. Verma SK, Ranjan R, Kumar V, et al. (2014) Wat1/pop3, a Conserved WD Repeat Containing Protein Acts Synergistically with Checkpoint Kinase Chk1 to Maintain Genome Ploidy in Fission Yeast *S. pombe. PLoS ONE* 9: e89587.
23. Morris GM, Goodsell DS, Halliday RS, et al. (1998) Automated docking using a Lamarckian genetic algorithm and an empirical binding free energy function. *J Comp Chem* 19: 1639-1662.
24. Pettersen EF,Goddard TD, Huang CC, et al. (2004) UCSF Chimera—a visualization system for exploratory research and analysis. *J Comp Chem* 25: 1605-1612.
25. Wallace AC, Laskowski RA, Thornton JM (1995) LIGPLOT: a program to generate schematic diagrams of protein-ligand interactions. *Protein Eng* 8: 127-134.
26. Chao WC, Kulkarni K, Zhang Z, et al. (2012) Structure of the mitotic checkpoint complex. *Nature* 484: 208-213.
27. Tange Y, Niwa O (2008) Schizosaccharomyces pombe Bub3 is dispensable for mitotic arrest following perturbed spindle formation. *Genetics* 179: 785-792.
28. Rischitor PE, May KM, Hardwick KG (2007) Bub1 Is a Fission Yeast Kinetochore Scaffold Protein, and Is Sufficient to Recruit other Spindle Checkpoint Proteins to Ectopic Sites on Chromosomes. *PLoS ONE* 2: e1342.
29. He X, Patterson T, Sazer S (1997) The Schizosaccharomyces pombe spindle checkpoint protein mad2p blocks anaphase and genetically interacts with the anaphase-promoting complex. *Proc Natl Avad Sci USA* 94: 7965-7970.

30. Dorer RK, Zhong S, Tallarico JA, et al. (2005) A small-molecule inhibitor of Mps1 blocks the spindle-checkpoint response to a lack of tension on mitotic chromosomes. *Curr Biol* 15: 1070-1076.
31. Mapelli M, Massimiliano L, Santaguida S, et al. (2007) The Mad2 conformational dimer: structure and implications for the spindle assembly checkpoint, *Cell* 131: 730-743.
32. Izawa D, Pines J (2012) Mad2 and the APC/C compete for the same site on Cdc20 to ensure proper chromosome segregation. *J Cell Biol* 199: 27-37.
33. Acharya BR, Chatterjee A, Ganguli A, et al. (2014) Thymoquinone inhibits microtubule polymerization by tubulin binding and causes mitotic arrest following apoptosis in A549 cells. *Biochimie* 97: 78-91.
34. Huzil J, Chen K, Kurgan L, et al. (2007) The roles of beta-tubulin mutations and isotype expression in acquired drug resistance. *Cancer Inform* 3: 159-181.

AIMS Press

© 2016 Shakil Ahmed et al., licensee AIMS Press. This is an open access article distributed under the terms of the Creative Commons Attribution License (http://creativecommons.org/licenses/by/4.0)